

Received November 29, 2020, accepted December 10, 2020, date of publication December 21, 2020, date of current version December 16, 2021.

Digital Object Identifier 10.1109/ACCESS.2020.3046364

# Underwater Spherical Shell Classification and Parameter Estimation Based on Acoustic Backscattering Characteristics

TIANYANG XU<sup>ID</sup>, XIUKUN LI<sup>ID</sup>, AND HONGJIAN JIA<sup>ID</sup>

Acoustic Science and Technology Laboratory, Harbin Engineering University, Harbin 150001, China

Key Laboratory of Marine Information Acquisition and Security, Ministry of Industry and Information Technology, Harbin Engineering University, Harbin 150001, China

College of Underwater Acoustic Engineering, Harbin Engineering University, Harbin 150001, China

Corresponding author: Xiukun Li (lixikun@hrbeu.edu.cn)

This work was supported in part by the National Natural Science Foundation of China (NSFC) under Grant 11774073 and Grant 51279033, and in part by the Open Project of State Key Laboratory of Acoustic, Chinese Academy of Sciences under Grant SKLA201904.

**ABSTRACT** Underwater quiet object detection and recognition by the target echo method is based on prediction and cognition of acoustic scattering characteristics. Spherical shell is a kind of common underwater quiet object whose scattering characteristics vary with the material, radius, and shell thickness. According to the acoustic scattering theory, we analyze the backscattering characteristics of vacuum spherical shell under different parameters and propose a method based on deep convolution neural network trained by backscattering morphological function to classify the objects and estimate the parameters. For the performance of shell material estimation, we compare the proposed deep learning method with the traditional classification method based on feature engineering, and the proposed method has better performance. For objects with different geometric scales, the estimation results of outer radius and shell thickness conform to the fitting formula based on medium frequency enhancement effect. The deep learning classification method based on acoustic scattering morphological function covers a large number of parameters by establishing a stable object feature library, and realize the accurate classification of underwater spherical shell objects.

**INDEX TERMS** Underwater objects, spherical shell, backscattering characteristics, deep convolutional neural network, classification.

## I. INTRODUCTION

Underwater quiet object detection and recognition is a challenging problem in underwater archeology and seabed exploration. In the process of sonar detection, there will be acoustic phenomena such as reflection and scattering when the transmitted signal meets the target. The mechanism of target acoustic scattering is complicated whereas researchers summarized it as a mathematical problem for physics described by wave equation and boundary conditions [1]. Research has shown that in the frequency range where the wavelength is equivalent to the target scale, the measured acoustic scattering characteristics can provide information for target recognition [2].

The associate editor coordinating the review of this manuscript and approving it for publication was Jiajia Jiang<sup>ID</sup>.

For objects with simple shapes, the complete theoretical solution of scattering field can be calculated by wave equation and boundary conditions [3], whereas it is difficult to obtain a strict theoretical solution for structures such as a finite-length cylinder or other complex shapes affected by the boundary conditions of cross-sectional [4]. Researchers often used the theoretical solution based on thin elastic shells to analyze the acoustic scattering phenomenon of a cylinder with finite length [5]. Since the acoustic scattering characteristics are related to the material, size, and structure of the object, and vary with the incident angle of sound waves as well as the environment where the target is located, it is necessary to extract the characteristics related to the object attributes as the basis for detection and recognition in practical applications. In this sense, it is significant to research the acoustic scattering characteristics of underwater objects. The time series and spectrum characteristics of target acoustic scattering signal

are the most basic characteristics [6]. With the development of resonance scattering theory, identifying resonance features in frequency spectrum has become an effective means for analyzing acoustic scattering signals [7].

With the improvement of calculation and experiment, it becomes possible to obtain the characteristics of scattered echoes under different incident angles of sound waves. By comparing the consistency between the experimental and calculated results in the time and the frequency domain, researchers used the time-angle spectrum and frequency-angle spectrum to analyze the scattering characteristics of the target [8]. Since the backscattered echo varies with the incident angle of the sound wave, different components appears under the condition of different incident angles, thereby the type of echo component can be identified according to the transformation law [9]. Li *et al.* studied an underwater water-filled cylindrical shell characteristics by the structural finite element coupled with acoustic finite element method [10]. Based on the highlight model, Wu *et al.* proposed a target scattering extraction and classification method based on Wigner-Ville distribution [11]. Dmitrieva identified materials based on the time delay of the secondary reflection using broadband sonar pulses [12].

The deep learning method forms the category or feature which represents the target attribute by characterizing the internal law of the sample data, which originated from the neural networks [13] in early stage. Due to the defect of local optimal value [14], the development of deep learning is limited until Hinton proposed the deep belief network (DBN), which set off the upsurge of deep learning development. Since then, convolutional neural network (CNN), recurrent neural network (RNN), and other network structures appeared. Deep learning has achieved research results in computer vision [15], speech recognition and natural language processing [16], [17], acoustic scene analysis [18], and other fields. In recent years, researchers have introduced deep learning methods into the classification and recognition of underwater target acoustic signals. Kamal *et al.* applied the DBN to the classification and recognition tasks of underwater passive targets, and achieved a higher recognition rate than traditional methods [19]. Jin proposed a method to realize accurate multiclass underwater target recognition by connecting sonar-echoscope and CNN. The mini-batch gradient descent in his research based on transfer learning performed better than traditional feature-based method [20]. Song combined the image enhancement and region-based CNN to recognize underwater creatures, and improve the performance on a small dataset [21]. Cao *et al.* combined the second-order pooling with CNN to obtain classification information from the time-frequency representation of acoustic signals [22]. The pattern of combining the research in the field of underwater acoustics with deep learning provides inspiration for the research content of this article.

According to the theoretical solution for the scattering field of a simple underwater object, this paper proposes a classification method for spherical shell objects based on deep

learning method by analyzing the morphological function and establishing the relationship between signal characteristics and target characteristics. First, we simulate the scattering characteristics of the underwater spherical shell's acoustic scattering. Then, we generate the object scattering data under different parameters according to the acoustic scattering theory and build a deep neural network model. Classify the materials and estimate the radius and thickness of underwater spherical shell. Finally, we evaluate the performance of the model proposed in the article and compare with the baseline method.

This paper is organized as follows: Section II describes the basic acoustic scattering theory. Section III provides the simulation analysis of underwater spherical shells. Section IV describes the model structure and data generation progress. In Section V, we explain the details of model training, metric evaluation, and the baseline method. This paper ends with concluding remarks in Section VI.

## II. BASIC THEORY OF UNDERWATER SPHERICAL SHELL OBJECTS

Spherical objects (including rigid spheres, flexible spheres, elastic spheres and spherical shells with different fillings and thicknesses) are the typical underwater target shapes whose acoustic scattering characteristics have been deeply studied. Due to the simple shape of spherical shell, the rigorous theoretical solution of acoustic scattering is easy to obtain. Through the study of basic shapes, we can explain the physical mechanism of acoustic scattering from elastomers, and clarify the fluctuation phenomenon of fluid-solid interface involved in scattering. We can use the obtained rigorous solution as a benchmark for other rigorous or approximate methods. This section first introduces the rigorous theoretical solution of elastic spherical shell scattering. We can use the normal series solution to calculate the scattering field of a vacuum spherical shell and elaborate the basic characteristics of acoustic scattering echoes.

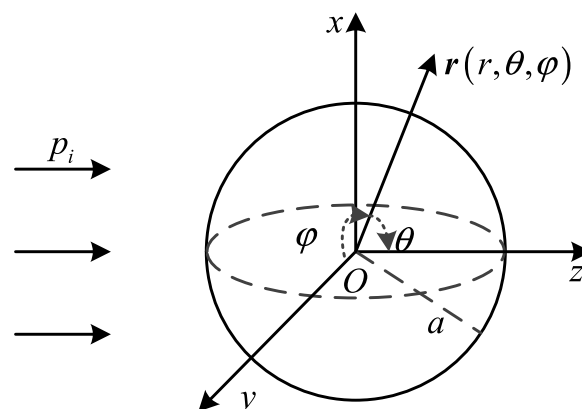


FIGURE 1. The schematic diagram of the scattering from a spherical object.

Fig. 1 reveals the acoustic scattering of a sphere with a plane wave incidence. The center of the sphere to be analyzed

is set as the origin of the spatial spherical coordinate system, where the radius of the sphere is  $a$ . The plane wave is incident on the sphere along the axis  $z$ , and the acoustic scattering echo varies with the change of the receiving position  $\mathbf{r}(r, \theta, \varphi)$ . Both the incident wave and the scattering wave are independent of azimuth angle  $\varphi$  and symmetrical with  $\theta$ . Without considering the effect of amplitude and time delay, the incident plane wave can be expressed as  $e^{ikz} = e^{ikr \cos \theta}$ , according to the spherical wave decomposition, we can obtain the following expression:

$$p_i = e^{ikr \cos \theta} = \sum_{n=0}^{\infty} i^n (2n + 1) j_n(kr) P_n(\cos \theta) \quad (1)$$

where  $j_n(\cdot)$  is the spherical Bessel function of order  $n$  and  $P_n(\cdot)$  is the Legendre function of order  $n$ . For the scattering wave, the solution dependent on  $r$  in the spherical coordinate takes the first kind of spherical Hankel function  $h_n^{(1)}(kr)$ . Without considering the time delay, the scattering wave can be expressed as:

$$p_s = \sum_{n=0}^{\infty} i^n (2n + 1) b_n h_n^{(1)}(kr) P_n(\cos \theta) \quad (2)$$

where  $b_n$  is the undetermined scattering coefficient, which will be determined by the boundary conditions of the sphere.

When the target is an elastic spherical shell, we must consider the boundary conditions of the inner wall, and at the same time, the acoustic field of the spherical shell will contain the spherical Neumann function  $y_n(\cdot)$ . Under different filling conditions, the boundary conditions are different. If the spherical shell is filled with fluid, there will be 6 boundary conditions for the inner and outer walls. If the inside of the spherical shell is vacuum, the number of boundary conditions will be reduced to 5. The radius of the shell is set as  $b$ , suppose that the inner space of  $r < b$  is filled with fluid. Then we can express the acoustic field in the spherical shell as:

$$\begin{aligned} \Phi &= \sum_{n=0}^{\infty} i^n (2n + 1) P_n(\cos \theta) [c_n j_n(k_{d2} r) + d_n y_n(k_{d2} r)] \\ \psi &= \sum_{n=0}^{\infty} i^n (2n + 1) P_n(\cos \theta) [e_n j_n(k_{s2} r) + f_n y_n(k_{s2} r)], \\ & \quad b \leq r \leq a \end{aligned} \quad (3)$$

The coefficients  $c_n$  and  $d_n$  as well as  $e_n$  and  $f_n$  are dual in spherical shell solution, the difference is only that the functions  $j_n(\cdot)$  and  $y_n(\cdot)$  are interchanged. Then the inner field of the spherical shell will be:

$$p_1 = \sum_{n=0}^{\infty} i^n (2n + 1) P_n(\cos \theta) g_n j_n(k_1 r), \quad r < b \quad (4)$$

where  $k_1 = \omega/c_1$ ,  $k_{d2} = \omega/c_{d2}$ ,  $k_{s2} = \omega/c_{s2}$ ,  $c_{d2}$ ,  $c_{s2}$  are the longitudinal wave velocity and transverse wave velocity of the elastic spherical shell respectively. The scattering

coefficient  $b_n$  solved from the boundary conditions can be expressed as:

$$b_n = -B_n/D_n \quad (5)$$

In the case that the inside of the spherical shell is vacuum,  $B_n, D_n$  are the 5 order determinant [23].

In order to eliminate the influence of object relative distance and propagation phase factor in acoustic scattering analysis, we can use the morphological function to describe the far-field scattering characteristics of objects, which is defined as follows:

$$f(x, \theta) = \left(\frac{2r}{a}\right)^{1/2} \frac{p_s(x, \theta)}{p_i(x)} e^{-ikr} \quad (6)$$

Morphological function is the response of the object to the incident wave. When the polar angle  $\theta = \pi$ , we can obtain the backscattering morphological function. According to the definition, the far field backscattering morphology function of spherical objects can be described as:

$$|f(x, \pi)| = \frac{2}{x} \left| \sum_{n=0}^{\infty} (-1)^n (2n + 1) b_n \right| \quad (7)$$

where  $b_n$  is determined by the boundary conditions of the sphere. In this paper, we mainly discuss the backscattering characteristics of elastic spherical shells.

### III. SIMULATION ANALYSIS OF UNDERWATER SPHERICAL SHELL OBJECTS

In this section, we discuss the influence of parameter changes on the characteristics of target scattering signals. For the spherical elastomer whose material and parameter of geometric size are given. According to (7), we can calculate the backscattering characteristics by the normal series solution. Table 1 gives the physical parameters of the materials involved in the theoretical calculation in this paper. Suppose that the inside of the shell is filled with air.

TABLE 1. The physical parameters of the simulation materials.

Material	Density (kg/m <sup>3</sup> )	Longitudinal wave velocity (m/s)	Transverse wave velocity (m/s)
Water	1000	1500	0
Stainless Steel	7900	5940	3100
Aluminum	2700	6350	3100
Air	1.29	331	0

Taking the stainless steel spherical shell as an example, the outer radius of the shell is 0.25m, the shell thickness is 5mm, and the observation frequency range of 0-100 kHz are separated by the step size of 100 Hz. Through the theoretical simulated calculation, Fig. 2(a) shows the backscattering morphology function of a stainless steel elastic spherical shell with a radius of 0.25m and a shell thickness of 5 mm. The abscissa of Fig. 2(a) represents the dimensionless frequencies  $ka$ , where  $k$  is the wavenumber of the incident sound and

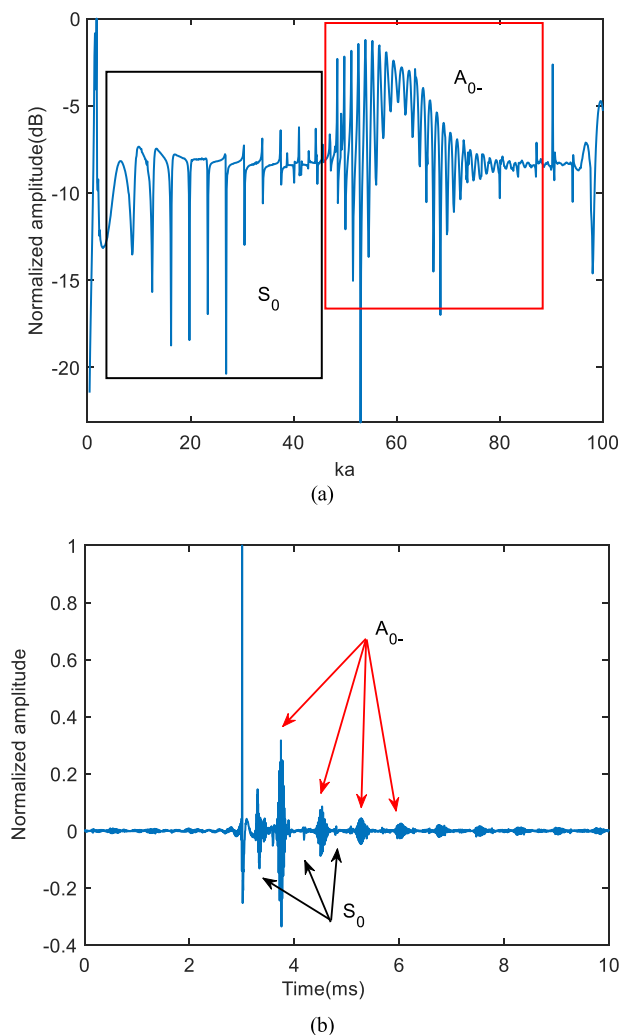


**FIGURE 2.** The simulation result of the simulated objects. (a) Backscattering morphology functions. (b) The waveform.

$a$  is the sphere radius. In addition, the ordinate represents the target strength by normalized amplitude.

For the Fig. 2 (a), in the low frequency range (marked by the black rectangular), the backscattering morphology function has an approximately periodic formants, and the amplitude of the formants is small, which is mainly composed of  $S_0$  waves (low-order symmetric Lamb waves) cause. In the mid-frequency (marked by the red rectangular), the backscattering morphology function shows the mid-frequency enhancement effect, mainly caused by the leakage of the shell surface (low-order subsonic asymmetric Lamb wave) [24]. The change of the backscattering morphology function is more complicated, and the amplitude has obvious maximum and minimum changes with frequency. In addition, as the frequency increases, the amplitude of the morphology function changes more drastically.

We can obtain the waveform of object backscattering echo by calculating the inverse Fourier transform on the backscattering morphology function, as shown in Fig. 2(b). When the target is an elastomer, there would be a series of elastic

acoustic scattering echoes after the specular reflection echo. The first one that appears is the strong specular reflection echo, followed by several wave packets. In the time domain, the  $S_0$  waves appear at equal intervals, but the amplitude is much smaller than that of the specular reflection echo. The  $S_0$  waves will easily submerge in the ambient noise in actual observation. Therefore, we cannot use the  $S_0$  wave as an effective component in observing backscatter characteristics. The wave packets of the  $A_{0-}$  wave appear in order, and the amplitude is constantly weakened due to the attenuation of energy during the propagation, but it is still greater than the amplitude of the  $S_0$  wave. In practical applications, the energy contained in these wave packets is relatively large, which can provide the most obvious signal characteristics available for detection and identification except for the mirror reflection echo, and is an effective radiation mode for underwater target acoustics scattering.

The backscattering morphology function of the elastic spherical shell is related to the material, radius and shell thickness of the spherical shell. Fig. 3 shows the comparison results of backscattering morphology functions under different parameters. Referring to the parameters in Fig. 3(a), the thickness, material, and radius of the shell are respectively changed, and the results are in Fig. 3(b)-3(d). The abscissa represents the dimensionless frequencies  $ka$ , where  $k$  is the wavenumber of incident sound and  $a$  is the sphere radius.

Compared with Fig. 3(a), the acoustic scattering morphology function in Fig. 3(b) shows that when the outer radius of the spherical shell remains unchanged and the thickness increases, the formants aroused by the  $A_{0-}$  wave becomes narrower and moves toward the low frequency. When the geometric parameter is fixed and the object material is aluminum, the resonant structure caused by the  $S_0$  wave and  $A_{0-}$  wave will change. The resonant structure of the  $A_{0-}$  wave moves to the high frequency direction, as shown in Fig. 3(c). When the object radius increases to 0.5m, only the presence of the  $S_0$  wave resonance structure can be observed, and the  $A_{0-}$  wave formants disappears in Fig. 3(d).

Theoretical and experimental have proved that the mid-frequency enhancement in the morphological function is an effective acoustic characteristic related to the inherent properties of the object. In practical applications, it can provide obvious characteristics available for detection and recognition except for specular reflection echo. The frequency range of mid-frequency enhancement is related to the shell material. That is, in case of different object parameters, the backscattering morphology functions will appear in different spectral characteristics, therefore we can use the backscattering morphology function as the basis for material classification and parameter estimation. In addition, we can apply the deep learning methods to discover the high-level abstract characteristics of the target acoustic scattering function.

#### IV. DEEP CONVOLUTIONAL NEURAL NETWORKS

In this paper, we used the one-dimensional (1D) backscattering morphology function as the input of the network.

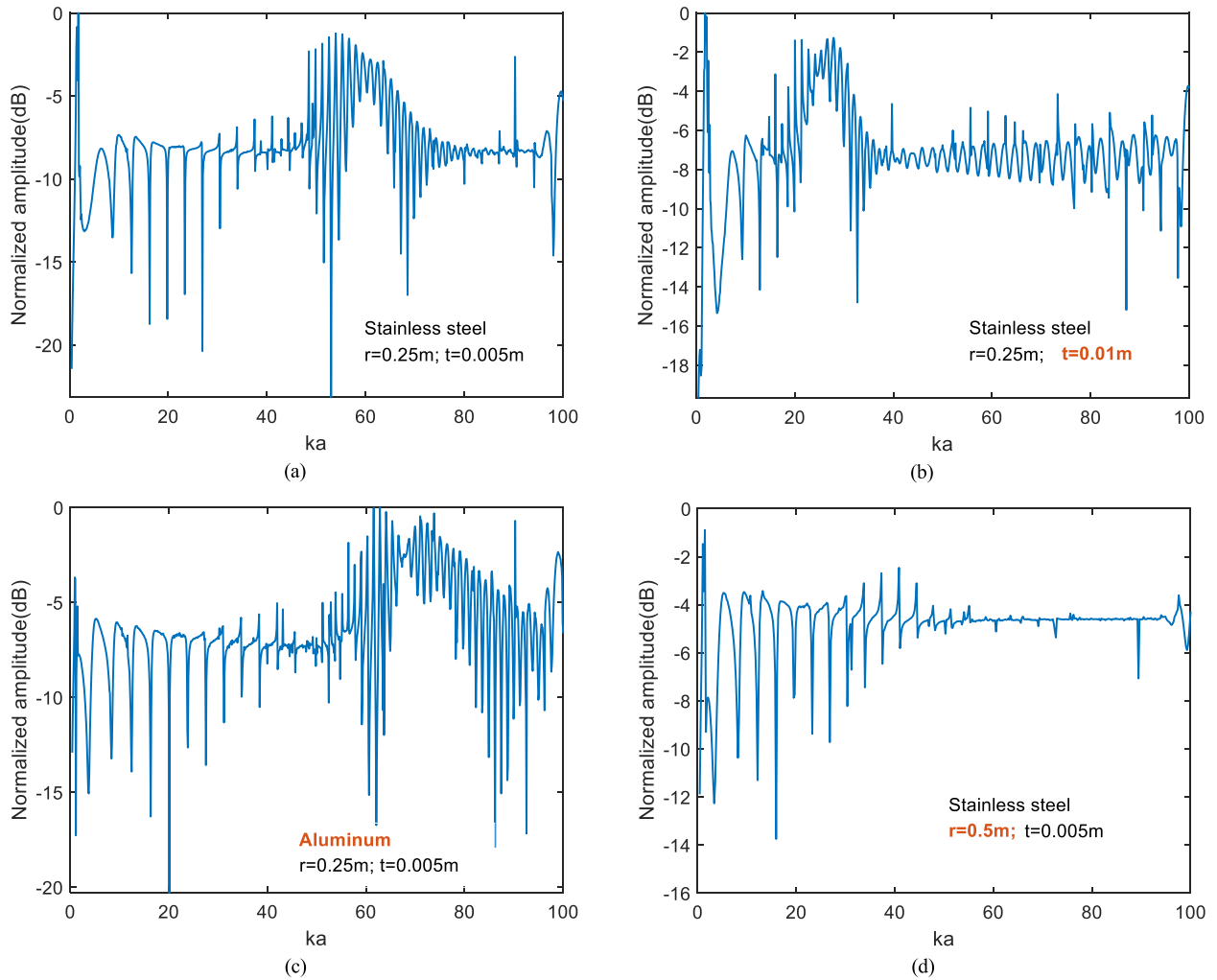


**FIGURE 3.** Comparisons of backscattering morphology function with different parameters. (a) Stainless steel shell with  $r = 0.25\text{m}$  and  $t = 0.005\text{m}$ . (b) Stainless steel shell with  $r = 0.25\text{m}$  and  $t = 0.01\text{m}$ . (c) Aluminum shell with  $r = 0.25\text{m}$  and  $t = 0.005\text{m}$ . (d) Stainless steel with  $r = 0.5\text{m}$  and  $t = 0.005\text{m}$ .

Although fully connected neural networks have demonstrated superior results in dealing with 1D input, considering the number of parameters of the network model, we applied the 1D-CNN to complete the classification and estimation tasks. Fu pointed out that it is difficult to learn the weights in fully connected layers to generate high and low frequency parts of a waveform simultaneously, while fully convolutional layers can preserve the local information and spatial arrangement of previous features well [25]. At present, some waveform-in and waveform-out models such as SEGAN [26] and GlotNet [27] adopt CNN structure to enforce the network to focus on temporally close correlations of the input signal.

Although the backscattering morphology function does not appear as a waveform in the time domain, its formant intervals and fluctuation changes between adjacent formants are similar to the variations of neighbor points in the waveform. Thus, 1D-CNN can be applied to extract formant features under different parameters well. Furthermore, researchers found that 1D-CNN has a better performance of inhibiting

over-fitting than fully connected layers in lower signal-to-noise ratio (SNR) cases in the training process. In addition, the number of training parameters and training time can be reduced as well.

#### A. DATA GENERATION

The backscattering characteristics of elastic objects are strongly dependent on the incident sound waves, which can excite more formants at higher frequencies. In order to obtain more object characteristic information and facilitate signal processing, it has great advantages to use extremely narrow pulse signals as transmitted signals. However, the energy of extremely narrow pulses is finite, which limits the working distance and has high requirements for transducers. Therefore, it has not been widely used in actual sonar engineering.

In object detection and recognition of active sonar, chirp signal is a kind of common signal form. Because of its large time-bandwidth product, it can obtain higher gain when using traditional pulse compression for signal detection, so it is

widely used in ranging, direction finding and some other applications. For underwater objects, stronger acoustic scattering will occur in a certain frequency band. Therefore, by studying the signals covering the specific frequency band, we can explain the scattering characteristics clearly and improve the detection and recognition performance effectively. Chirp signal can satisfy the above characteristic and it is easy to implement.

The entire observation frequency band is from 100 Hz to 100 kHz, which is wide enough to observe the resonance structure of the objects studied in this paper. The bandwidth of the transmitted signal is fixed at 50 kHz, whereas the initial frequency starts at 1000 Hz and increase in steps of 1000 Hz. The scanning method above can cover the entire observation frequency band and increase the amount of data. In this paper, we divided the material of the objects into two types. The radius varies from 0.24m to 0.52m with a step of 0.02m and the thickness varies from 3mm to 32mm with a step of 1mm. Then the amount of sample dataset will be  $15 \times 30 \times 100$ . Furthermore, we add noise with different SNR to each dataset to improve the noise generalization ability of the model.

**TABLE 2. Network configuration.**

Layer	Channel	Kernel Size	Stride	Padding	Output Size
Conv1	16	32	2	15	512*16
+RELU					
Conv2	32	32	2	15	256*32
+RELU					
Conv3	64	32	2	15	128*64
+RELU					
Conv4	128	32	2	15	64*128
+RELU					
Conv5	256	32	2	15	32*256
+RELU					
Conv6	1	1	1	-	32*1
+RELU					
Linear	1	-	-	-	N

## B. MODEL STRUCTURE

When we use a deep neural network for training, as the number of network layers increases, the weights, thresholds and parameters in the network will increase sharply, resulting in a corresponding increase in the complexity of the model. The layered training mechanism can reduce the time complexity of the model. In this paper, we designed the 1D-CNN network model to train the generated data. Table 2 shows the details of the network configuration in this paper. The model consists of six convolutional layers and uses a rectified linear unit (ReLU) as the activation function. The ReLU function alleviates the gradient disappearance of neural network to a certain extent, and accelerates the convergence speed of gradient descent. Among the convolutional layers of the network, the first five layers are with the same kernel, stride, and padding, whereas the feature channels will double in the next layer. The channel, kernel size, and stride are all set as one in the sixth convolutional layer to reduce the feature dimension.

For the last layer, we use the fully connected (FC) layer with linear activation to get the final output of size N, where N is the number of classes (Regression,  $N = 1$ ; Classification,  $N = 2$ ). Moreover, for the classification model, the output layer uses sigmoid activation to classify more than one class.

During training progress, the over-fitting is easy to occur in the lower SNR cases. Thus, we also incorporated the regularization method in the network to prevent over-fitting by introducing the dropout layers and  $L_2$  weight regularization. Fig. 4 shows the schematic diagram of the mode designed in this paper.

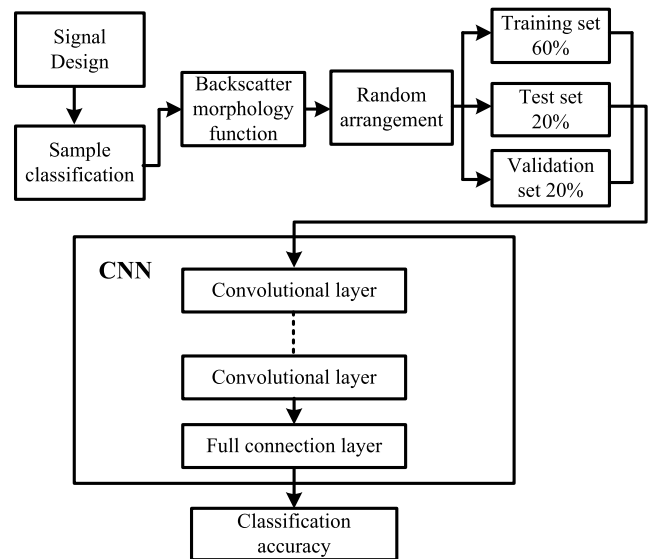


**FIGURE 4. Spherical shell target classification model based on the convolutional neural network.**

## V. EXPERIMENTAL RESULT

In the designed deep neural network, we apply the backscattering morphological function as the input of the model. Each dataset consists of 45000 noise-free samples with 1024 sampling points. In the designed network, the cross-entropy loss function and the adam optimizer are applied. Research found that a small learning rate is necessary in order to ensure the model converges smoothly. Therefore, the initial learning rate is set to 0.0001. The dropout probability is set to 0.5. In order to test the model performance that varies with the SNR, we add random noise from 0dB to 20dB to the clear dataset by a step of 5dB, and finally generate 5 group of datasets with different SNR. We divide each dataset according to the proportion of 60% training dataset, 20% validation dataset and 20% test dataset.

There is a strategy to train the model in this paper. We use the dataset with SNR 20dB to train the first model, and initialize the weights of all the layers by Xavier initialization. When the network converges stably, the model parameters will be saved as the initial parameters of other models trained by datasets under lower SNR, which is similar to the weight pre-training process. The advantage of the strategy is that the

model will have the memory of learning the primitive features of clear samples when we train the model with dataset in case of lower SNR. It can ensure certain stability of the features learned by the model, even if the sample is in larger noise. In addition, the losses are easier to converge at low SNR.

**A. MATERIAL CLASSIFICATION**

In this paper, we mainly consider two kinds of materials of the elastic spherical shells, which are the stainless steel and the aluminum. Therefore, we can regard the problem as a binary classification task. According to the analysis in Section II, the backscattering morphology function has different structures for objects under different parameters, so we can use the one-dimensional backscattering morphology function as the model input.

The baseline method uses auditory features such as Mel-Frequency Cepstral Coefficients (MFCC), Gammatone Cepstral Coefficients (GtCC), spectral centroid, spectral decrease, spectral crest, and spectral entropy to train an support vector machine (SVM) classifier. The total dimension of the features is 30. We use the classification accuracy as the evaluation index of the model. The classification accuracy rate varied with SNR presented in Fig. 5 shows the performance of the proposed network model.

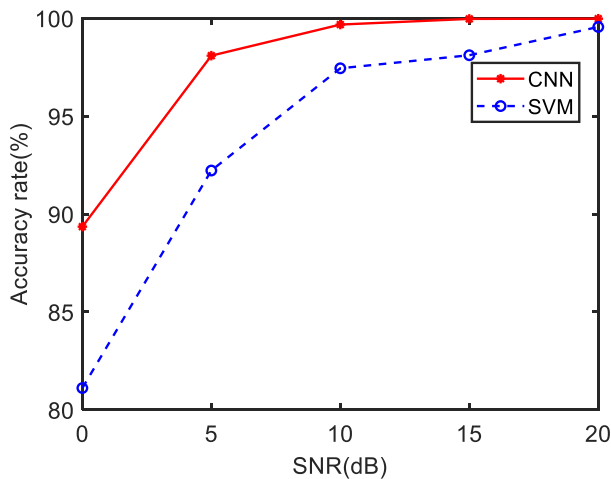


FIGURE 5. Material classification accuracy varied with SNR.

We can observe from Fig. 5 that the baseline method achieves a relatively higher classification accuracy rate of the object material varied with the increase of SNR. Even if the SNR is 0dB, the accuracy rate can reach 80%. Whereas in comparison, the proposed CNN method achieves a better and more stable accuracy rate overall, especially at 20dB, the accuracy rate reaches 100%.

**B. RADIUS AND THICKNESS ESTIMATION**

Radius and thickness are important geometric features that represent the physical properties of spherical shells. In the early research of the ray acoustics theory, the relationship between the backscattered echoes of the object incident with

continuous short pulses was discovered [3]. Researchers have proved that the incident wave frequency  $f_c$  with the maximum amplitude of the first  $A_{0-}$  wave is related to the radius-thickness-ratio, which can be used to estimate the radius and thickness of the object, whereas it is difficult to obtain the  $f_c$  in practical application. In response, Li proposed two approximate equations to evaluate the radius and thickness of a thin spherical shell [28] as shown in (8) and (9).

$$a = \frac{\sqrt{F_2^2 + 4F_1\omega_p\Delta t_{0l}} - F_2}{2F_1\omega_p} \tag{8}$$

$$h = \frac{ac}{E_1\omega_p a + E_2c} \tag{9}$$

where  $E_1 = 0.8001$ ,  $E_2 = 2.9587$ ,  $F_1 = 4.6514 \times 10^{-3}$ , and  $F_2 = 4.2544$ . These values will depend on the material of object shell and the surrounding medium. These two equations need to measure the frequency of greatest enhancement  $\omega_p$  and the echo delay  $\Delta t_{0l}$  in practice.

In this section, we train the regression model based on CNN to estimate the radius and thickness of the object, and compare the performance to the baseline method [28]. The parameters in (8) and (9) need to satisfy two conditions:

- (1). The object is stainless stain thin spherical shell;
- (2). There should be complete mid-frequency enhancement formants in the backscattering morphology function.

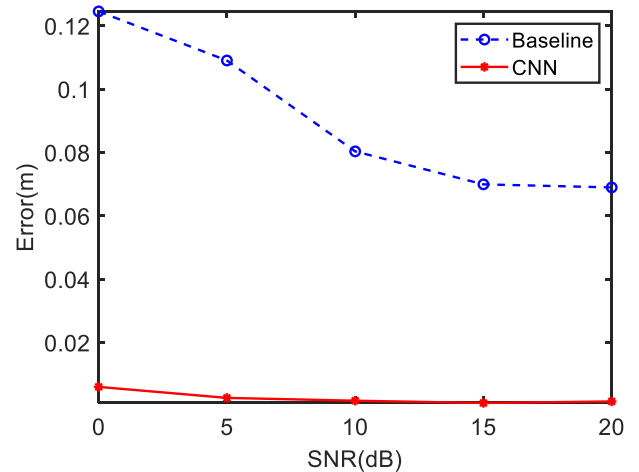


FIGURE 6. The error of radius varied with SNR.

Thus, we use the samples that satisfy the conditions to test the performance of the baseline method. Fig. 6 and Fig. 7 show the estimation error curve of radius and thickness varied with SNR in respectively. We use the absolute error to evaluate the estimation performance and use (10) to calculate the estimated error  $e$ ,

$$e = |x - \hat{x}| \tag{10}$$

where  $x$  is the real thickness or radius value of test dataset, and  $\hat{x}$  is the estimated value.

We can observe from Fig. 6 and Fig. 7 that the whole error of the baseline method is higher than that of the

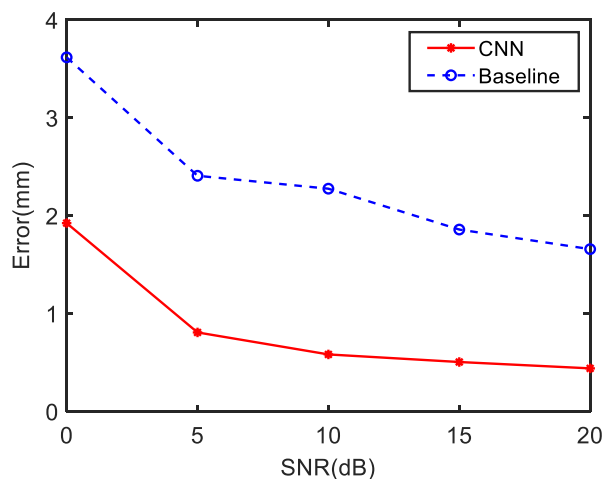


FIGURE 7. The error of thickness varied with SNR.

proposed CNN method. The reason is that for the baseline method, there would be extra errors introduced by extracting the values of  $\omega_p$  and  $\Delta t_{0l}$ , especially at low SNR cases. In addition, the accuracy of thickness is also influenced by the accuracy of the radius, and there will be error accumulation in estimating the thickness. The method based on proposed CNN structure achieves superior performance to the baseline method and it is more robust to noise.

## VI. CONCLUSION

Aiming at the problem of classification and recognition of underwater spherical shell objects, this paper proposes a convolutional neural network to train the acoustic scattering morphological function and estimate the radius and thickness of the elastic spherical shell. Through theoretical simulation, the backscattering morphological function of the target model is calculated and used as the input of the neural network to extract the deep characteristic information in the backscattering morphological function. Construct datasets with different SNR to evaluate the model. Whether the classification of material or the estimation of parameter, the performance of proposed classification method based on CNN is better than the baseline method, and it is robust to noise. Therefore, the model trained by neural network can be used as a stable and reliable feature library to characterize underwater spherical shell objects with different parameters, and provide theoretical and technical support for underwater target detection and recognition.

## REFERENCES

- [1] W.-L. Tang, J. Fan, Z.-C. Ma, *Acoustic Scattering of Underwater Target*. Beijing, China: Science Press, 2018, pp. 14–49.
- [2] D. P. Williams, “Fast target detection in synthetic aperture sonar imagery: A new algorithm and large-scale performance analysis,” *IEEE J. Ocean. Eng.*, vol. 40, no. 1, pp. 71–92, Jan. 2015, doi: 10.1109/JOE.2013.2294532.
- [3] L.-G. Zhang, N.-H. Sun, and P. L. Marston, “Midfrequency enhancement of the backscattering of tone bursts by thin spherical shells,” *J. Acoust. Soc. Amer.*, vol. 91, no. 4, pp. 1862–1874, Apr. 1992, doi: 10.1121/1.403716.
- [4] M. Tran-Van-Nhieu, “Scattering from a finite cylindrical shell,” *J. Acoust. Soc. Amer.*, vol. 91, no. 2, pp. 670–679, Feb. 1992, doi: 10.1121/1.402528.
- [5] G.-Y. Zheng, J. Fan, and W.-L. Tang, “Acoustic scattering from a fluid-filled finite cylindrical shell in water: I. Theory,” *Chin. J. Acoust.*, vol. 2011, vol. 30, no. 2, pp. 288–300, Aug. 2011, doi: 10.15949/j.cnki.0217-9776.2011.03.009.
- [6] A. Malarkodi, D. Manamalli, G. Kavitha, and G. Latha, “Acoustic scattering of underwater targets,” in *Proc. Ocean Electron. (SYMPOL)*, Oct. 2013, pp. 127–132, doi: 10.1109/SYMPOL.2013.6701922.
- [7] A. L. España, K. L. Williams, and D. S. Plotnick, “Acoustic scattering from a water-filled cylindrical shell: Measurements, modeling, and interpretation,” *J. Acoust. Soc. Amer.*, vol. 136, no. 1, pp. 109–121, Jul. 2014, doi: 10.1121/1.4881923.
- [8] A. M. Gunderson, A. L. España, and P. L. Marston, “Spectral analysis of bistatic scattering from underwater elastic cylinders and spheres,” *J. Acoust. Soc. Amer.*, vol. 142, no. 110, pp. 110–115, Jul. 2017, doi: 10.1121/1.4990690.
- [9] Y.-Y. Ding, F.-J. Shen, and F.-Y. Yuan, “Target spectral lines separation based on maximum likelihood method,” in *Proc. IEEE 23rd Int. Conf. Digital Signal Process. (DSP)*, Shanghai, China, Nov. 2018, pp. 1–5, doi: 10.1109/ICDSP.2018.8631875.
- [10] J. Li, T. Li, X. Zhu, and Y. Han, “Numerical study on vibration characteristics of the underwater partially fluid-filled cylindrical shell,” in *Proc. IEEE 8th Int. Conf. Underwater Syst. Technol., Theory Appl. (USYS)*, Wuhan, China, Dec. 2018, pp. 1–5, doi: 10.1109/USYS.2018.8778928.
- [11] Y. Wu, X. Li, and Y. Wang, “Extraction and classification of acoustic scattering from underwater target based on Wigner-Ville distribution,” *Appl. Acoust.*, vol. 138, pp. 52–59, Sep. 2018, doi: 10.1016/j.apacoust.2018.03.026.
- [12] M. Dmitrieva, K. Brown, G. Heald, and D. Lane, “Material recognition based on the time delay of secondary reflections using wideband sonar pulses,” *IET Radar, Sonar Navigat.*, vol. 13, no. 11, pp. 2034–2040, Nov. 2019, doi: 10.1049/iet-rsn.2018.5493.
- [13] J. J. Hopfield, “Neural networks and physical systems with emergent collective computational abilities,” *Proc. Nat. Acad. Sci. USA*, vol. 79, no. 8, pp. 2554–2558, 1982, doi: 10.2307/12175.
- [14] M. Bianchini and F. Scarselli, “On the complexity of neural network classifiers: A comparison between shallow and deep architectures,” *IEEE Trans. Neural Netw. Learn. Syst.*, vol. 25, no. 8, pp. 1553–1565, Aug. 2014, doi: 10.1109/TNNLS.2013.2293637.
- [15] S. Ren, K. He, R. Girshick, and J. Sun, “Faster R-CNN: Towards real-time object detection with region proposal networks,” *IEEE Trans. Pattern Anal. Mach. Intell.*, vol. 39, no. 6, pp. 1137–1149, Jun. 2017, doi: 10.1109/TPAMI.2016.2577031.
- [16] H. Purwins, B. Li, T. Virtanen, J. Schlüter, S.-Y. Chang, and T. Sainath, “Deep learning for audio signal processing,” *IEEE J. Sel. Topics Signal Process.*, vol. 13, no. 2, pp. 206–219, Apr. 2019, doi: 10.1109/JSTSP.2019.2908700.
- [17] J. Liao, T. Liu, M. Liu, J. Wang, Y. Wang, and H. Sun, “Multi-context integrated deep neural network model for next location prediction,” *IEEE Access*, vol. 6, pp. 21980–21990, 2018, doi: 10.1109/ACCESS.2018.2827422.
- [18] S. Adavanne, A. Politis, J. Nikunen, and T. Virtanen, “Sound event localization and detection of overlapping sources using convolutional recurrent neural networks,” *IEEE J. Sel. Topics Signal Process.*, vol. 13, no. 1, pp. 34–48, Mar. 2019, doi: 10.1109/JSTSP.2018.2885636.
- [19] S. Kamal, S. K. Mohammed, P. R. S. Pillai, and M. H. Supriya, “Deep learning architectures for underwater target recognition,” in *Proc. Ocean Electron. (SYMPOL)*, Oct. 2013, pp. 48–54, doi: 10.1109/SYMPOL.2013.6701911.
- [20] L. Jin, H. Liang, and C. Yang, “Accurate underwater ATR in forward-looking sonar imagery using deep convolutional neural networks,” *IEEE Access*, vol. 7, pp. 125522–125531, 2019, doi: 10.1109/ACCESS.2019.2939005.
- [21] S. Song, J. Zhu, X. Li, and Q. Huang, “Integrate MSRCR and mask R-CNN to recognize underwater creatures on small sample datasets,” *IEEE Access*, vol. 8, pp. 172848–172858, 2020, doi: 10.1109/ACCESS.2020.3025617.
- [22] X. Cao, R. Togneri, X. Zhang, and Y. Yu, “Convolutional neural network with second-order pooling for underwater target classification,” *IEEE Sensors J.*, vol. 19, no. 8, pp. 3058–3066, Apr. 2019, doi: 10.1109/JSEN.2018.2886368.

- [23] G. C. Gaunard, D. Brill, H. Huang, "Signal processing of the echo signatures returned by submerged shells insonified by dolphin 'clicks': Active classification," *J. Acoust. Soc. Amer.*, vol. 103, no. 3, pp. 1547–1557, 1998, doi: [10.1121/1.421302](https://doi.org/10.1121/1.421302).
- [24] S. D. Anderson, "Space-time-frequency processing from the analysis of bistatic scattering for simple underwater targets," Ph.D. dissertation, G.W. Woodruff School Mech. Eng., Georgia Inst. Technol., Atlanta, GA, USA, 2012.
- [25] S. Fu, Y. Tsao, X. Lu, and H. Kawai, "Raw waveform-based speech enhancement by fully convolutional networks," in *Proc. Asia-Pacific Signal Inf. Process. Assoc. Annu. Summit Conf. (APSIPA ASC)*, Dec. 2017, pp. 6–12, doi: [10.1109/APSIPA.2017.8281993](https://doi.org/10.1109/APSIPA.2017.8281993).
- [26] H. Phan, I. V. McLoughlin, L. Pham, O. Y. Chén, P. Koch, M. De Vos, and A. Mertins, "Improving GANs for speech enhancement," *IEEE Signal Process. Lett.*, vol. 27, pp. 1700–1704, 2020, doi: [10.1109/LSP.2020.3025020](https://doi.org/10.1109/LSP.2020.3025020).
- [27] L. Juvola, B. Bollepalli, V. Tsiaras, and P. Alku, "GlotNet—A raw waveform model for the glottal excitation in statistical parametric speech synthesis," *IEEE/ACM Trans. Audio, Speech, Language Process.*, vol. 27, no. 6, pp. 1019–1030, Jun. 2019, doi: [10.1109/TASLP.2019.2906484](https://doi.org/10.1109/TASLP.2019.2906484).
- [28] W. Li, G.-R. Liu, and V. K. Varadan, "Estimation of radius and thickness of a thin spherical shell in water using the midfrequency enhancement of a short tone burst response," *J. Acoust. Soc. Amer.* vol. 118, no. 4, pp. 2147–2153, Oct. 2005, doi: [10.1121/1.2040027](https://doi.org/10.1121/1.2040027).



**TIANYANG XU** was born in Harbin, Heilongjiang, China, in 1991. He received the B.S. degree from the College of Underwater Acoustic Engineering, Harbin Engineering University, Harbin, China, in 2014, where he is currently pursuing the Ph.D. degree. His research interests include target detection and recognition, pattern recognition, and underwater signal processing.



**XIUKUN LI** was born in Harbin, Heilongjiang, China, in 1962. She received the B.S. and M.S. degrees in electronic information engineering from Harbin Engineering University, in 1989, and the Ph.D. degree in 2000.

From 2000 to 2001, she was a Visiting Professor with the Norwegian University of Science and Technology. She is currently a Professor with the College of Underwater Acoustic Engineering, Harbin Engineering University, China. She has published a monograph and over 80 articles. Her research interests include underwater acoustic engineering, underwater target detection and recognition, and acoustic signal processing.

Dr. Li is a member of the Chinese Society of Physical Oceanography.



**HONGJIAN JIA** was born in Tieli, Heilongjiang, China. She received the B.S. degree from the College of Underwater Acoustic Engineering, Harbin Engineering University, Harbin, China, in 2015, where she is currently pursuing the Ph.D. degree. From 2019 to 2020, she was exchanged with Tampere University, Finland. Her research interests include underwater signal processing, target detection and recognition, and speech signal processing.

• • •